Disproving the Existence of Photons

André Malz,[1]

[1] *malz.correspondence@gmail.com* [https://orcid.org/0009-0007-0801-369X]

Abstract:

This article presents a comprehensive study that furnishes compelling evidence bolstering the notion of electromagnetic field continuity, accomplished through the implementation of a self-heterodyne measurement technique.

The primary objective was to investigate the detection method of FMCW for extremely weak signals, reaching energy levels akin to photons. Through thorough examination, significant contradictions emerged, favoring classical field theory and challenging the notion of electromagnetic field quantization. To strengthen this claim, a carefully designed experiment was conducted to measure sub-photon energy levels. The comprehensive analysis of both theoretical insights and experimental data presents compelling evidence, demonstrating the untenability of a quantized model for the electromagnetic field. These findings have profound implications for understanding the continuity of the electromagnetic field, prompting further exploration in this field of research.

1. Introduction

A scientific manuscript that challenges the existence of photons is understandably poised to encounter substantial resistance. Over the span of more than a century, the presence of photons has been established through an array of experiments. Or has it? The straightforward response is an emphatic negation. The experiments often cited as validating the existence of photons essentially affirm the discrete nature of interactions between fields and matter. The phenomenon of the photoelectric effect serves to illustrate that the absorption of energy from the field is inherently quantized. Additionally, Max Planck's work demonstrates that interactions with the electric field exclusively occur in quantized units, as to avert the "ultraviolet catastrophe." What remains unproven by these experiments, however, is the assertion that the quantized absorption or emission of energy into the electromagnetic field inherently results in the sustained retention of such quantized energy within said field. The presumption of a quantized electromagnetic field has persistently rested as an unsupported postulation. Similarly, the Compton effect, often attributed as the "proof" for the particle-like nature of photons, solely highlights the discretization of interactions. In instances where matter assimilates energy from the field and this assimilation takes place in discrete units of $E = h\nu$, a corresponding exchange of momentum $p = E/v = h\nu/c = h/\lambda$ emerges in adherence to momentum conservation principles, owing to the velocity of electromagnetic waves equating to the speed of light. This, however, does not substantiate the existence of discrete entities ("photons"), but rather stems from the governing law of momentum conservation. While this work does not challenge the proven discrete nature of interactions in these experiments, it does question the existence of photons, which remains unproven within the context of these experiments.

Frequency-Modulated Coherent Wave (FMCW) detection is a well-established measurement technique used in many fields, such as optical coherence tomography and LiDAR. While FMCW is explained by classical field theory, understanding its operation at the quantum-mechanical level presents challenges. One significant challenge in FMCW LiDAR is that it has the capability of detecting single photons, but the detection is based on frequency, which changes over time. This raises the question of whether a photon would change its frequency over its course [1].

Photons, unless subjected to redshift, blueshift, or reflection from a moving target, remain impervious to alterations in their frequency. The work conducted by Barber et al., in its ultimate reckoning, does not furnish an elucidation for the modus operandi of the measurement principle.

Instead, they make reference to a separate publication authored by Winzer et al. [2]. In this cited work, the authors arrive at a pivotal conjecture: "Thus, in a heterodyne system, the classical electromagnetic field quantities are added according to Maxwell's equations and the sum is detected, only then we can speak of a photon stream." Essentially, this embodies the solitary avenue through which the principles underpinning FMCW measurements can be comprehended, preserving validity even when dealing with energy magnitudes considerably less than $h\nu$. In point of fact, this declaration inherently signifies that "the electromagnetic field preserves continuity, with the term 'photon' finding relevance exclusively upon detection." According to the purview advanced by this study, photons merely epitomize the dynamic interplay between the field and matter, relinquishing their existential claims during the course of field propagation - a phenomenon exclusively attributed to Maxwellian propagation. Regrettably, the authors veer from this paradigm by erroneously grafting the concept of uncertainty onto domains where its applicability is unwarranted.

In Barber et al.'s study, they managed to measure energy down to the scale of two photons. Interestingly, they didn't delve further into the concept of photons, and consequently, they didn't endeavor to measure energy in quantities smaller than a single photon. This appears perplexing given the principles of FMCW operation. In FMCW, each measurement period is made up of numerous smaller measurements. The measured energy is linked to the entirety of this measurement period. To put it differently, if the researchers had focused on just a quarter of the measurement period's energy, they would have effectively measured what could be thought of as half a "photon" (imagining very tiny units of energy), provided they averaged the measurements accordingly. This missed opportunity could have prompted a deeper reexamination of our understanding of photons and energy measurement.

This study aims to explore the possibility of measuring energy units smaller than a single photon and seeks to elucidate the interpretation of such measurement outcomes.

2. Detection principle of FMCW

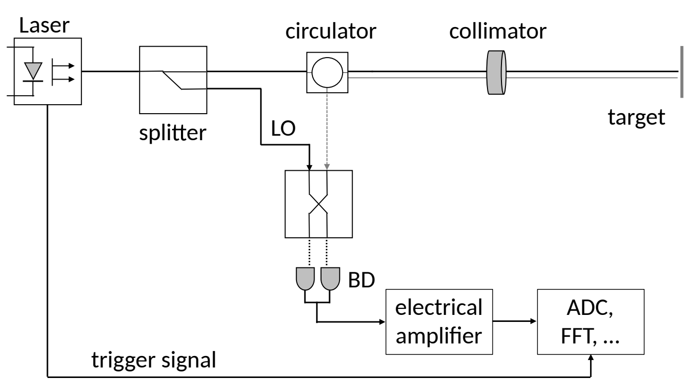

Fig. 1. Typical setup for Frequency-Modulated Continuous Wave (FMCW) LiDAR detection

Figure 1 illustrates a typical setup for FMCW LiDAR detection. The system consists of a swept-source laser, which is divided into two paths: the local oscillator (LO) and the signal path. The optical signal transmitted through the signal path interacts with a target and subsequently combines with the LO signal on a balanced detector (BD). The resulting signal is then amplified using an electrical amplifier before being digitized and processed. Additionally, to mark the initiation of the chirps generated by the laser system, a trigger signal is provided by the laser, which facilitates the capture of the time series of measurements at the detector.

At the detector, the field strengths of the local oscillator (LO) and the signal reflected from the target combine, resulting in their classical observation. The detector measures the intensity of the combined signals, which corresponds to the absolute square of the field strength. Due to the sweeping nature of the laser and the round-trip propagation time of the signal to and from the target, the frequencies of the combined signals are not identical. As a consequence, a beat signal is generated, characterized by a frequency significantly lower than the optical frequencies of the laser signal, and it is sampled by the detector. Typical sampling frequencies utilized in FMCW LiDAR systems fall within the range of 1GHz. The energy of the squared field strength can be quantified in terms of photons and the resultant signal can be mathematically represented as follows:

$$i_{bd}(t) = \frac{2\eta q}{T}\sqrt{N_{LO}N_{sig}}\cos(2\pi\kappa\tau t + \phi) + i_s(t) \tag{1}$$

In Equation 1, the variable κ represents the linear chirp of the laser with its associated chirp rate, τ corresponds to the round trip time, η denotes the quantum efficiency of the detector, q signifies the elementary charge, ϕ represents a fixed phase, and N_{sig} and N_{LO} denote the number of photons in the signal and local oscillator, respectively. The signal is subject to noise $i_s(t)$, primarily stemming from the shot noise of the local oscillator.

For an LO photon flux much larger than the signal flux, $i_s(t)$ is a Gaussian random process with zero mean and variance

$$\sigma^2(t) = \frac{2\eta q^2}{T}BN_{LO} = \frac{\eta q^2}{T^2}len_{FFT}N_{LO} \tag{2}$$

It's important to note that in equation 2, the symbol B represents the bandwidth, not of the integration time, but rather of a single detection in the time domain, denoted as $T_{TD} = T/len_{FFT}$.

Equation 1 elucidates how the beat frequency is determined by a target located at a distance d, c represents the speed of light.

$$f_{beat} = \kappa\tau = \kappa\frac{2d}{c} \tag{3}$$

The extraction of distance information from the detected signal in the time domain can be achieved through the utilization of a Fourier transformation. To facilitate this process, the signal is multiplied by a window function, such as Hamming or Hanning, before undergoing Fourier transformation. The resulting frequency spectrum reveals the detected beat frequency, which directly corresponds to the distance information. It is important to note that for comprehensive coverage, the application of up- and down-chirps is employed to detect moving targets. This approach allows for the calculation of the frequency shift resulting from the Doppler effect in relation to the distance information. However, in the case of static targets located at fixed positions, the distinction between up- and down-chirps becomes inconsequential, and a single chirp is sufficient for accurate measurements.

The determination of the number of detected photons in the signal path can be achieved using the detected signal [1]. By averaging a large number of power spectra, the average of the resulting power spectra associated with the signal is directly proportional to the quantity $N_{LO}N_{sig}$, while the averaged noise floor is proportional to N_{LO}. Consequently, in a system limited by shot noise, the normalized averaged power spectra exhibit a noise floor value of 1. The value corresponding to the signal frequency in the normalized power spectra therefore represents:

$$sig_{fourier} = \eta N_{sig} \tag{4}$$

In Equation 4, η denotes the quantum efficiency, and N_{sig} represents the number of photons in the signal. The normalized signal strength in the shotnoise-limited system therefore corresponds to the number of detected photoelectrons plus 1.

In real FMCW systems there are further noise sources. While for strong LO signals the detector noise is less important, the noise of the electrical amplifier is not really negligible. Therefore, when detecting very small signal strengths, the following procedure can be followed: First, the average noise power of the amplifier is determined by disconnecting both LO and receive signal from the balanced detector. Then the average noise power of the LO is determined by connecting only the LO signal to the balanced detector. The noise power of the LO is determined from the now averaged noise power, minus the noise power of the electrical amplifier. To determine the signal strength in units of photon quanta, the obtained power spectra are averaged, from which the averaged noise of the electrical amplifier is subtracted, and the signal thus obtained is normalized by the LO noise. If further noise sources occur, they show up as a noise floor above the value "1". The signal value in photoelectrons is the signal value above that overall noise floor.

Materials and Methods

The objective of this experiment is to quantify energy levels within each measurement interval that fall below the magnitude of a single 'photon'. Initially, these measurements were carried out using standard FMCW target measurements. However, these FMCW measurements were subject to the presence of speckle, caused by the surface roughness of the target, resulting in a significant speckle contrast. To mitigate the impact of speckle, the experimental setup was streamlined to the configuration illustrated in Figure 2.

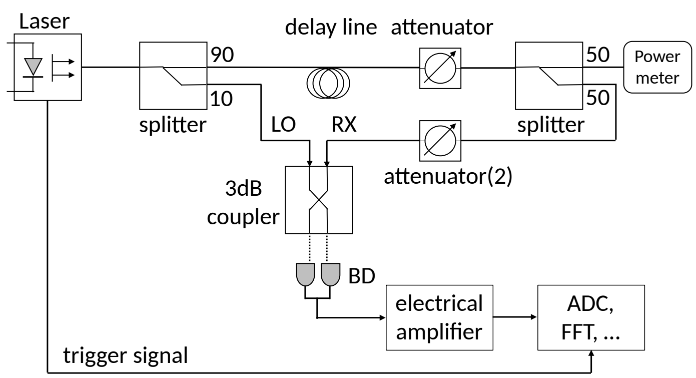

Fig. 2. Self-Heterodyne Measurement Configuration for Speckle Avoidance

The experimental setup is based on Bridger's swept source, which produces frequency sweeps (power 3.2mW at 1550nm) and triggers a detection board. The laser source is utilized as the swept source. For detection, a balanced detector (Thorlabs PDB570C) with a responsivity of $R = 1A/W$ and a quantum efficiency of $\eta = 0.8$ at 1550nm is employed, incorporating an integrated electrical amplifier. Given the feeble nature of the signal, an additional Low-Noise Amplifier (Nooelec LaNA HF) is introduced into the setup. The augmented analog signal is captured through a National Instruments DAQ system (NI PXIe-1082, NI PXIe-5763). All other elements within the setup are standard.

The frequency transition rate of the sweep is specified at 100GHz/s, generating two sweeps in both directions lasting approximately 35µs each. The sampling rate is set to 500MSamples/s.

To mitigate undesired noise, the optical gain was minimized, and the detection was set to the "Balanced" mode. This configuration was chosen instead of auto-balancing, as auto-balancing introduced additional noise that could not be reduced through averaging. The laser source generated up and down sweeps while triggering at each start. The acquisition system recorded 44,000 samples for each up and down sweep. From the recorded data, 16,384 samples were selected for each ramp, focusing on a region where the laser was clearly locked.

When dealing with measurements of weak signals, it becomes necessary to fine-tune the delay line to align the signal precisely with a single bin. This adjustment has the added advantage of enabling deliberate avoidance of a window function, which has the potential to modify the signal characteristics. Moreover, to facilitate examination of shorter measurement intervals, the bin number must be divisible by a factor representing a power of 2. In this context, the initial peak was aligned to a bin that is evenly divisible by 8.

Results

Acquired data, along with the corresponding signal processing, can be found in Dataset 1, [3].

Aside from the contribution of electrical amplifier noise, the performance of the setup is primarily constrained by shot noise. A residual, minor reflection might stem from the initial attenuator, which couldn't be entirely nullified even with the inclusion of an additional optical isolator. The noise baseline exclusively exhibits shot noise characteristics. This is achieved by eliminating the averaged electrical amplifier noise from both the signal and local oscillator, and subsequently normalizing the signal with the local oscillator noise. It's worth noting that there could be a slight remaining offset due to variations introduced by multiple measurements - reconnecting fibers may lead to marginal fluctuations in effective laser power. However, since this offset remains uniform, it can be rectified by intentionally scaling the noise baseline to a value of 1.

Given that the detector employed is an Avalanche Photodiode (APD), which inherently manifests excess noise, the noise baseline is not unity but rather represented as $F = M^i$, where M signifies the gain (M=2.5 for given detector at lowest gain) and i represents the excess noise index, which is specified as 0.3 for this particular sensor. Consequently, the count of photons within a bin is derived by normalizing the signal, subtracting 1, and subsequently scaling it with $M^i/\eta = 2.5^{0.3}/0.8 = 1.65$.

Upon significant averaging, static noise stemming from factors such as reflections and Analog-to-Digital Converter (ADC) noise may manifest. This static noise introduces an unvarying offset across all averaged measurements. In situations where distinct sets of averaged measurements are available, they can reciprocally function as local oscillator baselines for one another's signals. By subtracting the noise baseline from a measurement lacking any signal (pure noise) from another measurement conducted at a point where a signal is present, the outcome is the effective eradication of static noise. This operation leads to an amplification of shot noise by a factor of $\sqrt{2}$, while concurrently mitigating the presence of static noise.

Figure 3 illustrates that through ample averaging, the noise floor can be sufficiently smoothed, revealing signals with energy levels below that of a single photon.

Given that the displayed signal is a result of averaging, the current inquiry revolves around determining whether the input constitutes a quantized quantity, with the outcome reflecting an averaging of discrete values. Alternatively, it prompts us to consider whether the input signal is inherently continuous and causally aligns with the already-averaged value.

Discussion

The Fourier transform is a linear function. Therefore, for the Fourier transform of equation 1, the following holds true:

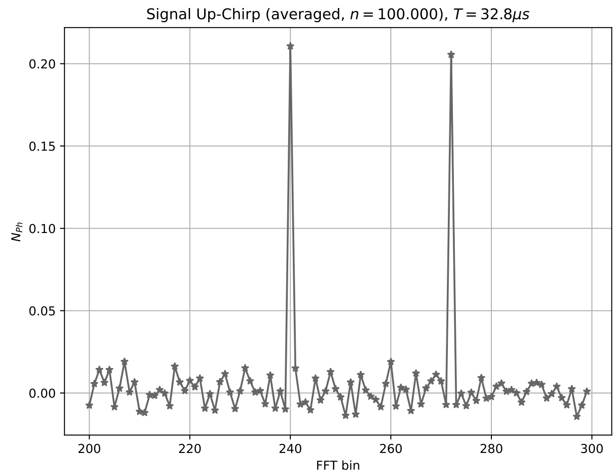

Fig. 3. Detection of Energy Levels Below One Photon per Measurement Interval

$$\mathcal{F}(i_{bd}(t)) = \mathcal{F}(\frac{2\eta q}{T}\sqrt{N_{LO}N_{sig}}\cos(2\pi\kappa\tau t + \phi)) + \mathcal{F}(i_s(t)) \tag{5}$$

Hence, in the discourse concerning signal generation, it becomes feasible to delineate the signal itself from the superimposed shot noise originating from the local oscillator.

The signal emerges when we perform a mathematical operation called the Fourier transform. This operation takes the data collected from the signal over a period of time and processes it using specific intervals. In this case, we're using 16,384 data points. Before applying this transformation, we already have 16,384 individual data points gathered in the time domain.

As per the current scientific understanding, when energy is released into the electromagnetic field, it stays contained within that field until it's detected. It doesn't get divided and spread across different measurements. Think of it like small packets of energy. These packets must be completely detected in a single measurement of time; they can't be split into parts.

The path where this detection occurs is labeled as 'RX' in Figure 1. At a certain point, it divides into two parts and then combines with another signal known as the local oscillator, or 'LO'. When there's only a tiny amount of energy, like a few 'photons', half of these 'photons' go to one detector, and the other half go to a different one. If we were to count these 'photons' as whole units, the count would follow a specific pattern described by Poisson statistics, with an average number determined by 'RX/2'. Only at specific moments when a 'photon' arrives, we observe an electron being detected. In all other instances, the count of detected electrons remains at zero, and there is no interaction between the signals.

Figure 4 illustrates a simulated scenario in which an average of 20 photoelectrons ($\eta = 1$) is detected. In this case, the signal conforms to a continuous behavior.

In Figure 5, we observe a simulated scenario in which only 100 photoelectrons are dispersed across the entirety of an FMCW measurement interval encompassing 200 samples. Consequently, the mean count per detection interval stands at 0.5. The resultant interference signal predominantly comprises a multitude of zeros.

Both figures also depict the signal in a non-quantized scenario. It's important to note that what's illustrated is solely the signal component of the comprehensive detected signal, which is still susceptible to the addition of noise from the local oscillator.

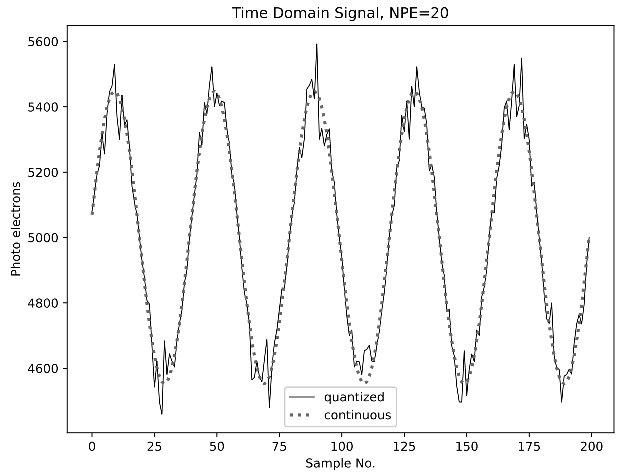

Fig. 4. Simulated Signal with Quantized Field: Average of 20 Photoelectrons per Sample

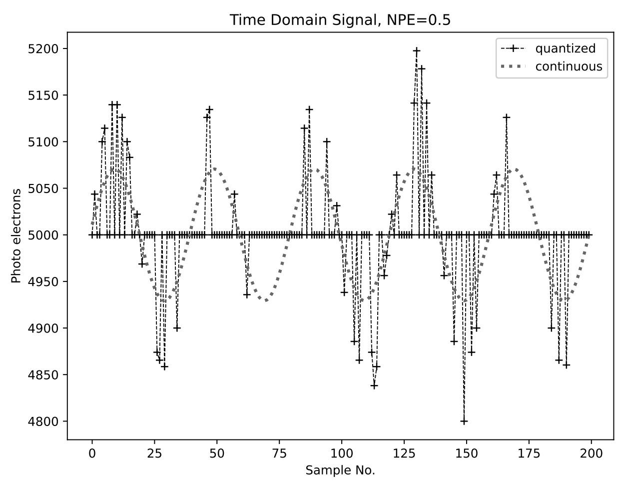

Fig. 5. Simulated Signal with Quantized Field: Average of 0.5 Photoelectrons per Sample

As the signal strength of the receive path diminishes, an increase in the occurrence of zeros becomes evident within the time-domain signal. Given the non-uniform nature of a sine signal, this phenomenon leads to a reduction in the count of detected photoelectrons for each received photoelectron. This simulation outcome for decreasing quantities of received photoelectrons is presented in Figure 6. The y-axis employs a square-root scale, revealing that halving the input energy corresponds to a roughly fourfold decrease in the detected number of photoelectrons.

Consequently, the apparent count of photoelectrons would consistently fall short of the actual

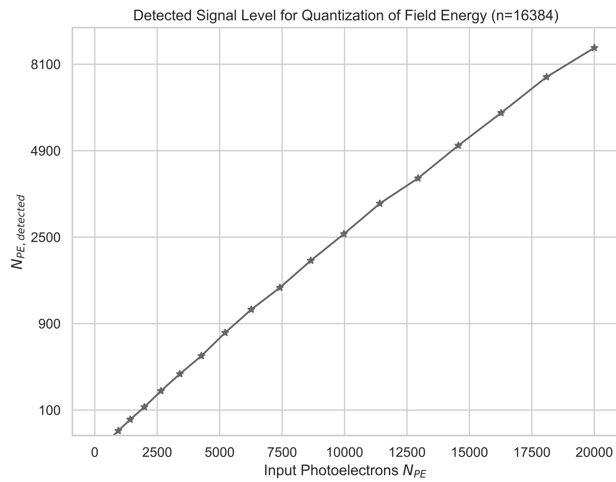

Fig. 6. Correlation Between Detected and Received Photoelectrons for Simulated Quantized Field Energy at Low Energy Levels (Note the Square Root Scale)

count within this detection scheme, particularly when the average photoelectron count per individual time domain detection dips into the single digits or even drops below one. Illustrating this effect, Figure 7 presents the attenuation of detected photoelectrons in relation to input photoelectrons, expressed in decibels (dB), across a comprehensive detection window comprising 16,384 values. Notably, as photon counts per detection interval decrease, the attenuation grows notably pronounced, ranging between 20 and 25 dB.

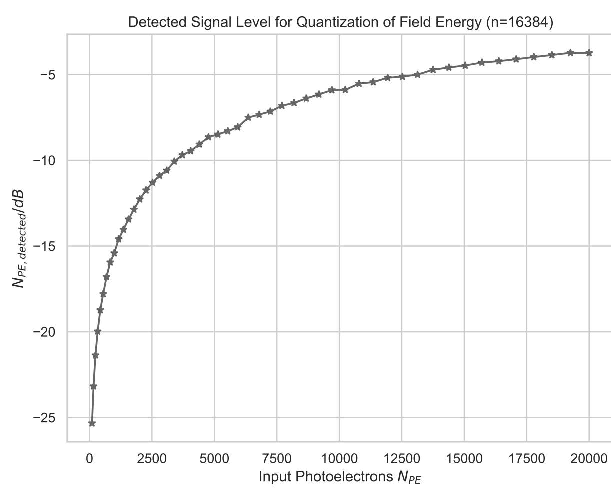

Fig. 7. Correlation between Detected and Received Photoelectrons for Simulated Quantized Field Energy at Low Energy Levels (Logarithmic Scale)

Nonetheless, such behavior remains absent in actual data observations, as depicted in Figure

8 (please note the linear scale). In instances where the signal energy in the receiving path is reduced, the detected photon count aligns with the diminishment in signal energy. There is just a constant factor of about 2 between the expected and measured values. Further exploration revealed that this is explainable: the measured laser power is an average of the laser output, while the power during the sweeps is lower. Additionally, alongside the coupling losses between the used attenuators, there is coupling loss to the detector, and another possibility is that the excess noise factor of the APD could be slightly higher. The detected energies clearly exhibit a linear relationship with input power, and they notably surpass the levels anticipated for the quantized scenario (roughly -25 dB relative to input power, as illustrated in Figure 7).

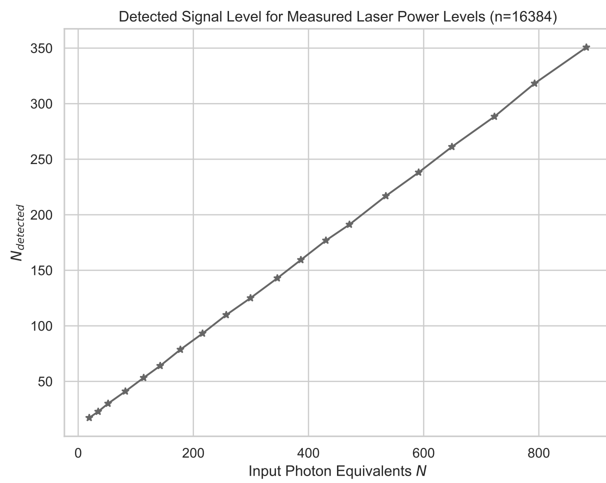

Fig. 8. Correlation between Detected and Received Photon Energy Equivalents at Low Energy Levels: Experimental Data (Linear Scale)

The linear relationship can be comprehended through the premise that the energy is uniformly spread across the measurement interval, aligning with the "continuous" curves in Figures 4 and 5. Furthermore, the energies detected in individual instances (i.e., per single time domain measurement) are significantly smaller than that of a single photon. It's also important to emphasize that the energies constituting the signal cannot stem from a solitary photon. This phenomenon is ascribed to the fact that the signal emerges from the interplay between two distinct frequency ramps - one from the local oscillator and the other from the signal itself. Crucially, the specific frequencies of both the local oscillator and the signal alter with each instance of time domain measurement.

Moreover, a coherent and uninterrupted signal would open avenues for scrutinizing energy distribution within narrower measurement intervals. If the measurement interval were divided in half, each measurement should theoretically encapsulate half the energy, provided signal continuity. The investigation of shortened measurement intervals can be streamlined by scrutinizing a reduced number of samples while preserving the same dataset. The ensuing outcome is illustrated in Figure 9, thereby affirming the existence of a uniformly distributed energy profile.

Table 1 presents vital measurements along with their associated confidence levels. The value of σ was computed as the square root of the variance present within the averaged noise floor.

Quantum mechanics attributes the Poisson distribution of photon events to the fundamental uncertainty principle. Consider a scenario where the target remains static. In such cases, the

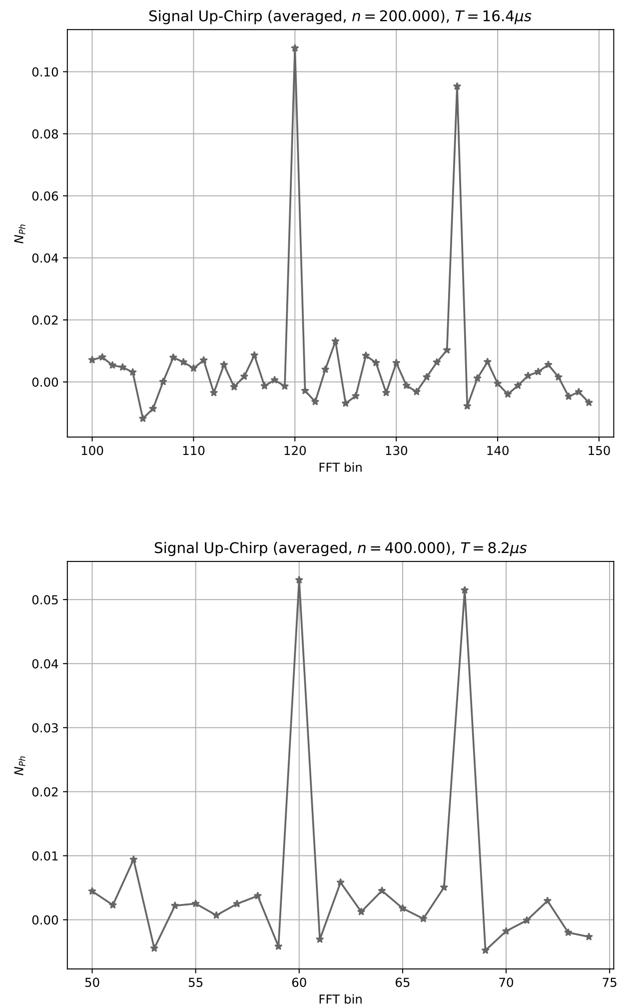

Fig. 9. Reduction in Measurement Interval Duration

frequency of a photon emitted toward the target remains unchanged until it reaches the detector. When the number of photons reaching the detector decreases, according to the uncertainty principle, the arrival time uncertainty should increase, leading to statistically different arrival times for photons of a specific frequency.

However, for accurately deriving the sine function, which eventually generates a distinct peak at the beat frequency, precise arrival times are imperative. This necessity arises from the dependence of the beat frequency on both the local oscillator's frequency and the signal photons' frequency at a specific moment. While an increased uncertainty in arrival times would typically result in a broadening of the frequency peak, empirical observations challenge this expectation. Notably, in real-world measurements, such broadening remains absent.

These observations suggest that we may not be dealing with discrete photons but instead with pure electromagnetic waves characterized by precise arrival times. It's worth noting that the uncertainty principle primarily applies when a detector records individual detections. The

Table 1. Signal Levels and Associated Confidence Intervals For Bin 240, Up-Chirp

Measurement Interval	$T = 32.768\mu s$	$T = 16.384\mu s$	$T = 8.192\mu s$
Number of Photons	0.21	0.11	0.053
σ	0.0091	0.0064	0.0047
confidence / σ	23.1	16.8	11.9

apparent reason for this uncertainty may be linked to the statistical process of energy accumulation until a sufficient amount of energy is available for a quantized detection from the field.

However, even if we set aside the aforementioned arguments and maintain a commitment to some form of averaging, according to a quantized model the incoming 'photons' per measurement interval also would need to adhere to Poisson statistics (additionally ignoring the fact they then would have to be detected also during several time domain detections, what is not possible for quantized entities per definition). Granted, the precise identification of the signal component within individual measurement intervals is confounded by the shot noise originating from the local oscillator. However, what can be established is a statistical overview encompassing numerous measurements. This statistical overview can then be contrasted with a simulation, both for the scenario involving Poisson statistics and that of a continuous, unchanging distribution of energy. To execute this comparison, a sequence of measurements is conducted to determine the average energy value. Subsequently, the distribution corresponding to this average value is simulated for both statistical scenarios. Given the substantial discrepancy between the two statistics, particularly when the averaged value of $\eta N/F$ falls within the range of 1...4, dedicated measurement series are devised to attain the requisite values.

The results of simulations conducted for specific values of $\eta N/F$ are illustrated in Figure 10. The signal statistics starkly align with the scenario of continuous energy distribution, thus contradicting the assumption of Poisson statistics.

This underscores that even in scenarios with a limited count of photons per measurement interval (again, disregarding the 'impossible' detection scheme spanning multiple time domain measurements), the signal level deviates from Poisson statistics. Instead, it exhibits a uniform energy distribution.

Conclusion

Through an objective exploration of Frequency-Modulated Continuous Wave (FMCW) measurements, particularly focusing on the realm of self-heterodyne measurements, it becomes evident that these methodologies are better suited to elucidate the nature of a continuous field as opposed to one that is discretized. This conclusion emerges from an unbiased analysis of the evidence at hand.

In situations involving exceedingly weak signals, a discretized field would undergo severe attenuation and fail to yield a detectable signal. However, measurement data clearly disproves this expectation by showing an absence of such attenuation. Instead, it strongly supports a continuous energy distribution, effectively refuting the concept of a quantized field. Upon closer examination of smaller measurement intervals, a notable trend emerges: the detected energy maintains a direct proportionality to the length of the detection interval. This observation provides additional compelling evidence in support of the continuous nature of the electromagnetic field. Last but not least, the statistical behavior of the signals aligns closely with a continuous energy distribution.

The phenomenon of quantization occurs both at the emission and detection stages of energy

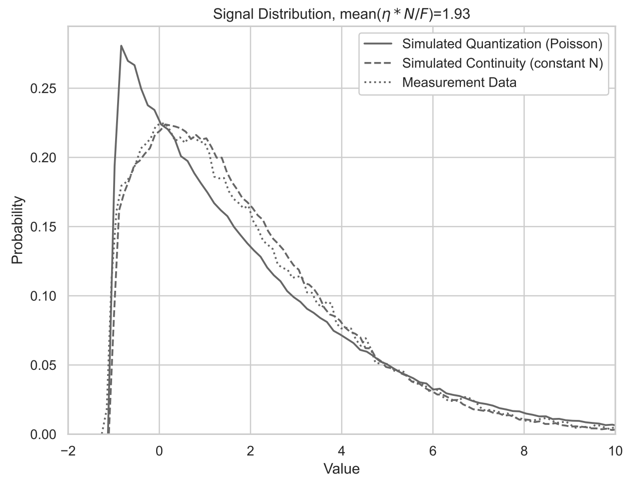

(a)

Fig. 10. Signal Statistics: Poisson and Continuous Signal Distribution, Along with Measured Data Statistics

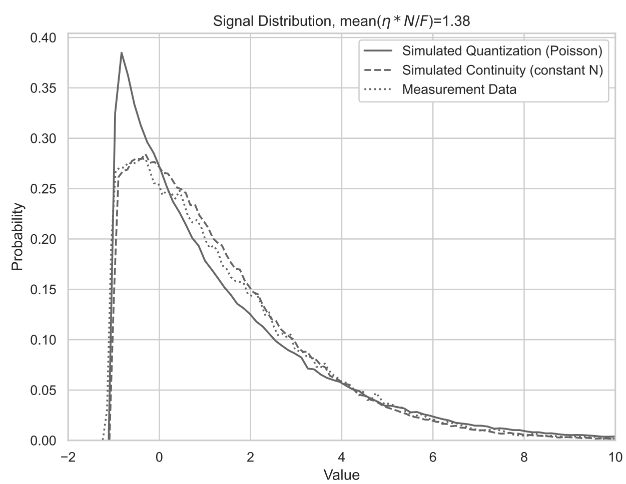

(b)

Fig. 10. (continued)

within the electromagnetic field. The electromagnetic field itself maintains continuity, adhering strictly to Maxwell's equations and the principles of superposition, even at low energy levels. Quantization is distinctively manifested during both emission and detection processes. When electromagnetic fields are coherently added, the sum of the fields is subject to quantization. However, there is no quantization in the electromagnetic field and there are certainly no 'photons'.

The precise mechanism governing the quantization process during both emission and detection within an otherwise continuous field stands as a compelling avenue warranting further exploration in research.

3. Disclosure

The author declares no conflicts of interest.

References

1. Z. W. Barber, J. R. Dahl, T. L. Sharpe, and B. I. Erkmen, "Shot noise statistics and information theory of sensitivity limits in frequency-modulated continuous-wave ladar," JOSA A **30**, 1335–1341 (2013).
2. P. J. Winzer and W. R. Leeb, "Coherent lidar at low signal powers: basic considerations on optical heterodyning," J. modern Opt. **45**, 1549–1555 (1998).
3. A. Malz, "Dataset for research paper "disproving the existence of photons"," (2023). figshare (2023), https://doi.org/10.6084/m9.figshare.24073172.v1.